Wide-band, band-pass and versatile Hybrid Filter Bank A/D conversion for software radio

Caroline Lelandais-Perrault, Tudor Petrescu, Daniel Poulton, Pierre Duhamel, Jacques Oksman

Wide-band, band-pass and versatile Hybrid Filter Bank A/D conversion for software radio

Caroline Lelandais-Perrault, Tudor Petrescu, Daniel Poulton, Pierre Duhamel and Jacques Oksman

***Abstract*—This paper deals with analog-to-digital (A/D) conversion for future software/cognitive radio systems. For these applications, A/D converters should convert wide-band signals and offer high resolutions. In order to achieve this and to overcome technological limitations, the A/D conversion systems should be versatile, i.e. it should be possible to adapt the conversion characteristics (resolution and bandwidth) by software. This work studies and adapts Hybrid Filter Banks (HFBs) in this context. First, HFBs, which can provide large conversion bandwidth, are extended to band-pass sampling, thus minimizing the sampling frequency. Then, we provide efficient ways of improving the HFB resolution in a smaller frequency band, only by reprogramming the digital part. Moreover, this study takes into account the main drawback of HFBs which is their very high sensitivity to analog imperfections. Simulation results are presented to demonstrate the performance of HFBs.**

***Index Terms*—Analog-to-digital conversion, hybrid filter banks, wide-band, band-pass, versatility, software radio, cognitive radio.**

I. Introduction

Future wireless systems will represent a real challenge as well as an outstanding opportunity over the next 10-20 years. A trend of using higher data rates (up to 1 Gb/s for instance) and high working frequencies can be noticed. Moreover, next generation mobile communications will have to deal with a wide range of different wireless access systems (e.g. various standards, applications). So-called "software radio" introduced in 1992 [1] comes from this need for versatile multi-standard terminals or base stations. Then the idea of cognitive radio was initiated [2] where the terminal explore the radio spectrum and determine the portion of the frequency band that may be used for the communication link.

To achieve software radio needs, several flexible receivers appeared [3] [4]. In these receivers, a first stage downconverts the appropriate communication channel. The signal is then converted in the digital domain through a classical A/D converter and finally digitally processed. These receivers are a step forward compared to traditional circuits that are individually customized. They receive one channel at arbitrary frequency with any modulation. But this solution does not make it possible to perform radio spectrum sensing which is required in cognitive radio systems. In these systems, the A/D converter should be placed ideally directly in RF without any frequency translation. Also, the A/D converter should be wide-band. As an example, the set of standards GSM, UMTS, GPS and WiFi implies the conversion of the frequency band from 880 MHz to 2.5 GHz. Regarding the required resolution, a 14-bit resolution is required for the GSM standard since a 9-bit resolution is sufficient for the WiFi standard. It is obvious that, considering the highest constraints, a 14 bit, 5 GS/s A/D converter is not realistic. Even if we knew

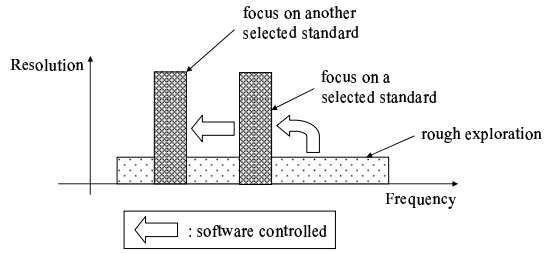

Fig. 1. Illustration of future A/D conversion versatility: frequency focusing

how to build such an A/D converter, its power dissipation would be overwhelming. So we must reconsider the A/D conversion in the cognitive radio context.

In order to satisfy the cognitive radio requirements, one interesting idea could be versatile A/D converters. Indeed, converting the whole band with a maximum resolution is certainly not necessary and would be a waste of energy. For example, the A/D converter could digitize the whole band at a rather low resolution. Once the software has explored the spectrum and found a band corresponding to pre-determined criteria, it could change the A/D converter parameters to improve the resolution in that particular band (Figure 1). We call this "frequency focusing".

In this work, we propose to study the Hybrid Filter Bank A/D converters and adapt them to the cognitive radio needs. The HFBs are multi-rate systems that use a 3-stage process: analog frequency band decomposition through an analysis filter bank; A/D conversion; and finally, digital reconstruction through a synthesis filter bank. HFBs are interesting because from a given sampling rate on each channel, it enlarges the conversion bandwidth. An HFB is said to be a "perfect reconstruction HFB" if its transfer function is a pure delay. But in reality, perfect reconstruction is not possible. So an HFB must be designed to approximate perfect reconstruction as closely as possible.

In the literature, some methods synthesize jointly the analog part and the digital part [5], [6] and [7]. These methods require the realization of given analog transfer functions which becomes increasingly difficult as monolithic integration dimensions decrease. Another class of synthesis methods starts from the knowledge of the analysis filter frequency responses and synthesizes the best digital part. Assuming that a calibration process makes it possible to know the analysis filter frequency responses, this technique relaxes the constraints upon the realization of the analog part. In [8], the author finds the synthesis filters by calculating the inverse FFT of the ideal synthesis filters frequency responses but this method doesn't offer to perform any tradeoff between frequencies.

In this article, we propose global least mean square synthesis methods that start from the knowledge of the analog frequency responses. Minimizing a criterion describing the near perfect reconstruction of the HFB, these methods can take account of the knowledge of the input signal and also a possible tradeoff between performance characteristics, all of which relax constraints upon the digital part.

As above, software radio applications will lead to the conversion of high frequency band-pass signals. So band-pass sampling should be studied in order to minimize the sampling frequency. Classical band-pass theory is here extended to the HFB case. Also, HFB synthesis methods are extended to the band-pass case.

Concerning versatility, the frequency focusing idea may be achieved in HFBs. Global least mean square synthesis methods have been adapted in order to synthesize digital filters so that the resolution is improved in a

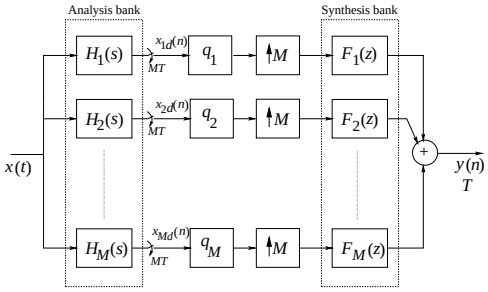

Fig. 2. Maximally decimated hybrid filter bank structure

smaller bandwidth. The software can therefore dynamically change the resolution of an HFB by reprogramming the digital filters with the appropriate set of coefficients.

In the software/cognitive radio context, high frequencies, high resolutions, low cost, achieving a robust architecture are a great challenge. This work shows the very high sensitivity of HFBs to the mismatch between their analog and digital parts. This confirms that the HFB design methods should work for any analog frequency response. In this respect, further research should be carried out into calibration techniques.

In Section II, the well-known perfect reconstruction equations are given. The main characteristics of HFBs are defined; i.e. distortion and aliasing. HFB design methods aimed at relaxing the analog design constraints are presented. Section III presents HFB adaptation to software/cognitive radio needs. First, the band-pass sampling for HFBs is presented and followed by the synthesis method to perform frequency focusing. Finally, robustness regarding analog versus digital mismatch is studied. Section II and III are illustrated with simulation results.

II. HFB A/D CONVERTERS THEORY AND DESIGN METHODS

A. Review of HFB theory

Figure 2 shows a maximally decimated HFB of M channels. $x(t)$ is the real input signal to be digitized at $1/T$ rate and $y(n)$ is the digital output of the HFB. $H_m(s)$ are the continuous-time analysis filter transfer functions and $F_m(z)$ are the discrete-time synthesis filters transfer functions, with $m \in \{1, 2, ..., M\}$. The blocks $q_1, ..., q_M$ are the branch quantizers. After analog filtering, the branch signals $x_m(t)$ are sampled at a rate of $1/MT$. Ignoring the quantizers, the Fourier transform of the HFB output signal $y(n)$ is [9], [10]:

$$Y(e^{\mathrm{j}\omega}) = \frac{1}{T}\sum_{p=-\infty}^{\infty} T_p(e^{\mathrm{j}\omega}) X\left(\mathrm{j}\Omega - \mathrm{j}\frac{2\pi p}{MT}\right) \quad (1)$$

with

$$T_p(e^{\mathrm{j}\omega}) = \frac{1}{M}\sum_{m=1}^{M} F_m(e^{\mathrm{j}\omega}) H_m\left(\mathrm{j}\Omega - \mathrm{j}\frac{2\pi p}{MT}\right), \quad (2)$$
$$\omega = \Omega T,$$

where $X(\mathrm{j}\Omega)$ is the Fourier transform of $x(t)$, Ω the pulsation and ω the normalized pulsation.

It is assumed that the input signal is strictly bandlimited to B. In this case, the Nyquist criterion for sampling with an effective sampling frequency of $1/T = 2B$ without aliasing is fulfilled. (1) can then be rewritten as follows:

$$Y(e^{\mathrm{j}\omega}) = \frac{1}{T}\sum_{p=-(M-1)}^{M-1} T_p(e^{\mathrm{j}\omega}) X\left(\mathrm{j}\Omega - \mathrm{j}\frac{2\pi p}{MT}\right) \quad (3)$$

because, for $-\pi < \omega \leq \pi$, only $2M-1$ terms have non zero contributions [10]. Perfect reconstruction means that the output $y(n)$ is only a scaled, delayed and sampled version of the input. Therefore, perfect reconstruction conditions will be [9], [10]:

$$T_p(e^{\mathrm{j}\omega}) = \begin{cases} ce^{-\mathrm{j}\omega\rho}, p = 0, \rho \in \mathbb{R}_*^+, c \in \mathbb{R}_* \\ 0 \qquad\quad , p \in \mathcal{P}. \end{cases} \quad (4)$$

where ρ is the overall HFB's delay, c is the scale factor and $\mathcal{P} = \{-(M-1), ... -1, 1, ..., M-1\}$.

B. HFB performance evaluation

The perfect reconstruction conditions cannot be achieved [5]. The HFB output signal consists of the input signal whose magnitude and phase are damaged, and additive parasitic aliasing signals, all of which limit the resolution of the system. As a remark, in this work, analog filters and A/D converters are supposed linear. So, we don't take into consideration nonlinear distortion like intermodulation (except quantization when precised).

We define two major performances to characterize the HFB quality reconstruction: the distortion function $R(\omega)$ given in (5) and the aliasing functions $T_p(e^{j\omega})$, $p \in \mathcal{P}$.

$$R(\omega) = \frac{T_0(e^{\mathrm{j}\omega})}{ce^{-\mathrm{j}\omega\rho}} \tag{5}$$

This distortion function has ideally a magnitude equal to 1 and a phase equal to 0.

Concerning aliasing, each $T_p(e^{j\omega})$, $p \in \mathcal{P}$, defines an aliasing transfer function for which it is possible to calculate mean and maximum values throughout the band. This leads to $2M-2$ values and complicates the comparison between two HFBs. We propose to calculate a synthesis of all aliasing functions. Considering aliasing terms as decorrelated noises, the total aliasing function consists in summing the powers of aliasing functions:

$$TotalAliasing(\omega) = \sum_{p \in \mathcal{P}} \left| T_p(e^{\mathrm{j}\omega}) \right|^2 \tag{6}$$

C. HFB implementation constraints

HFB design needs analog filters, elementary A/D converters and digital filters.

The digital part performances are essentially limited by the processing power and the calculation accuracy. Fortunately, technological progress will make it possible to push back these limitations. It will always be necessary, however, to minimize the size of the digital part in order to minimize both cost and power consumption.

A/D converters limitations are essentially the sampling frequency, the resolution and the input bandwidth. In the case of a direct RF conversion, the input bandwidth requirement is stronger than for an IF conversion. This is a technological aspect that concerns the sample and hold part of A/D converters.

Regarding the analog part, high frequency analog filter integration is tricky. The design of the analog part becomes increasingly difficult as the filter order or the quality factor become higher. And above all, manufacturing errors of passive components may be up to 20% and even more. Moreover, these errors change depending on ageing and temperature. Tuning is a possible solution to approach the desired analog filters transfer functions but this is a costly solution. Paragraph III-C1 shows that these phenomena affect HFB performance a lot.

Therefore the chosen strategy here is to maximally relax the realization of the analog part. To do that, the presented methods start from the knowledge of the frequency responses of the analog filters and calculate the corresponding digital filters in order to minimize the aliasing and the distortion. Thus, easily feasible bandpass analog filters can be chosen.

D. HFB design methods relaxing implementation constraints

The following methods calculate FIR synthesis filters. Therefore, their transfer functions are:

$$F_m(z) = \sum_{n=0}^{N-1} f_m(n) z^{-n}, \quad m \in \{1, 2, ..., M\}. \tag{7}$$

where $f_m(n)$ are the coefficients of the impulse response of digital filters. In this case, the synthesis problem is linear. So the coefficients may be found in a least square sense.

Eight-channel HFBs have been designed with the following methods. Paragraph II-E gives the results and compares the methods.

1) Least mean square local approximation HFB synthesis method (LMSLA): This method was first applied in [11]. We consider more general synthesis filter frequency responses $\mathcal{F}_m(\omega)$. (2) becomes:

$$\mathcal{T}_p(e^{\mathrm{j}\omega}) = \frac{1}{M}\sum_{m=1}^{M} \mathcal{F}_m(e^{\mathrm{j}\omega}) H_m\left(\mathrm{j}\Omega - \mathrm{j}\frac{2\pi p}{MT}\right), \quad (8)$$

Perfect reconstruction are:

$$\mathcal{T}_p(e^{\mathrm{j}\omega}) = \begin{cases} ce^{-\mathrm{j}\omega\rho}, p = 0, \rho \in \mathbb{R}_*^+, c \in \mathbb{R}_* \\ 0 \qquad\quad , p \in \mathcal{P}. \end{cases} \quad (9)$$

where ρ is the overall HFB's delay, c is the scale factor and $\mathcal{P} = \{-(M-1), ... -1, 1, ..., M-1\}$.

Considering K pulsation values ω_k equally distributed in $[-\pi, \pi]$, $\mathcal{F}_m(\omega_k)$ may be calculated by resolving the perfect reconstruction system. Then, each $\mathcal{F}_m(\omega)$ frequency response is approximated by a FIR filter $F_m(e^{\mathrm{j}\omega})$ frequency response.

Noting $\mathbf{f}_m$ the vector of coefficients for the m-th synthesis filter:

$$\mathbf{f}_m = [f_m(0), ..., f_m(N-1)] \quad (10)$$

For each branch m, the best filter coefficients values of $\mathbf{f}_m$ are obtained so that the actual frequency response fits the desired K-point values in the square error sense. The optimization algorithm is the standard Matlab one (namely Gauss-Newton). Paragraph II-E shows that the results are not satisfactory and can be much better using the global approximation methods that follow.

2) Least mean square global approximation HFB synthesis method - Discrete-frequency criterion (LMSGAD): This method has been presented in [12]. Perfect reconstruction conditions (4) are written for each of the K pulsation values equally distributed in $[-\pi, \pi]$ interval, using (2) for $T_p(e^{\mathrm{j}\omega})$ and (7) for $F_m(e^{\mathrm{j}\omega})$:

$$T_p(e^{\mathrm{j}\omega_k}) = \begin{cases} ce^{-\mathrm{j}\omega_k\rho}, p = 0, \rho \in \mathbb{R}_*^+, c \in \mathbb{R}_* \\ 0 \qquad\quad , p \in \mathcal{P} \end{cases} \quad (11)$$

$k \in \{1, 2, ..., K\}$, where:

$$T_p(e^{\mathrm{j}\omega_k}) = \frac{1}{M}\sum_{m=1}^{M} F_m(e^{\mathrm{j}\omega_k}) H_m\left(\mathrm{j}\Omega_k - \mathrm{j}\frac{2\pi p}{MT}\right). \quad (12)$$

with

$$\omega_k = \Omega_k T.$$

For a given ω_k, (11) is a system of $2M-1$ complex equations or, equivalently, $2 \times (2M-1)$ real equations. Hence, a linear system of $2 \times (2M-1) \times K$ real equations and $M \times N$ unknown variables results. For a matrix form of the above equation system, the definitions of different vectors follow:

$$\mathbf{e}(\omega) = \begin{bmatrix} 1 & e^{-\mathrm{j}\omega} & \cdots & e^{-\mathrm{j}(N-1)\omega} \end{bmatrix} \quad (13)$$

The vector of the FIR filter coefficients is:

$$\mathbf{f} = \begin{bmatrix} \mathbf{f_1} \cdots \mathbf{f_M} \end{bmatrix}^{\mathrm{T}} \quad (14)$$

where $\mathbf{A}^{\mathrm{T}}$ denotes the transpose of the matrix $\mathbf{A}$. The matrix of the shifted versions of all the analog filters $H_m(\mathrm{j}\Omega)$ with the elementary delays of the synthesis filters contribution is:

$$\mathbf{H}_K = \begin{bmatrix} \mathbf{H}(\omega_1) \\ \mathbf{H}(\omega_2) \\ \vdots \\ \mathbf{H}(\omega_K) \end{bmatrix}. \quad (15)$$

The matrix $\mathbf{H}(\omega)$ may be seen in (16) for typographic constraints. $H_m^{(p)}(\mathrm{j}\Omega)$ is the $2\pi p/MT$ shifted version of

$H_m(\mathrm{j}\Omega)$:

$$H_m^{(p)}(\mathrm{j}\Omega) = H_m\left(\mathrm{j}\Omega - \mathrm{j}\frac{2\pi p}{MT}\right). \tag{17}$$

With the following notation:

$$\mathbf{t}_K = \begin{bmatrix} \mathbf{t}(\omega_1) \\ \mathbf{t}(\omega_2) \\ \vdots \\ \mathbf{t}(\omega_K) \end{bmatrix} \tag{18}$$

where

$$\mathbf{t}(\omega) = cM \begin{bmatrix} e^{-\mathrm{j}\omega\rho} & 0 & \cdots & 0 \end{bmatrix}^{\mathrm{T}} \tag{19}$$

$$\mathbf{H_R} = \begin{bmatrix} \mathrm{Re}\{\mathbf{H_K}\} \\ \mathrm{Im}\{\mathbf{H_K}\} \end{bmatrix} \tag{20}$$

and

$$\mathbf{t_R} = \begin{bmatrix} \mathrm{Re}\{\mathbf{t_K}\} \\ \mathrm{Im}\{\mathbf{t_K}\} \end{bmatrix}, \tag{21}$$

the matrix form of the perfect reconstruction conditions written for the given set of frequency values is:

$$\mathbf{H_R f} = \mathbf{t_R}. \tag{22}$$

$\mathrm{Re}\{\mathbf{A}\}$ and $\mathrm{Im}\{\mathbf{A}\}$ denote respectively the real and the imaginary part of the matrix $\mathbf{A}$.

In the general case, the system (22) is overdetermined and inconsistent. However, a least square solution can be found [13]:

$$\mathbf{f} = (\mathbf{H_R}^{\mathrm{T}}\mathbf{H_R})^{-1}\mathbf{H_R}^{T}\mathbf{t_R} \tag{23}$$

which minimizes the square sum of the error vector (the error vector's Euclidean norm):

$$\mathbf{\Delta} = \|\mathbf{H_R f} - \mathbf{t_R}\|^2. \tag{24}$$

3) Least mean square global approximation HFB synthesis method - Continuous-frequency criterion (LMS-GAC): Approach the perfect reconstruction for a given pulsation consists in minimizing the following criteria:

$$J(\omega) = \|\mathbf{H}(\omega)\mathbf{f} - \mathbf{t}(\omega)\|^2 \tag{25}$$

where $\mathbf{H}(\omega)$, $\mathbf{f}$ and $\mathbf{t}(\omega)$ are defined above. (25) is equivalent to:

$$\begin{aligned} J(\omega) &= (\mathbf{H}(\omega)\mathbf{f} - \mathbf{t}(\omega))^{\dagger}(\mathbf{H}(\omega)\mathbf{f} - \mathbf{t}(\omega)) \\ &= \mathbf{f}^{\dagger}\mathbf{H}(\omega)^{\dagger}\mathbf{H}(\omega)\mathbf{f} - \mathbf{f}^{\dagger}\mathbf{H}(\omega)^{\dagger}\mathbf{t}(\omega) \\ &\quad - \mathbf{t}(\omega)^{\dagger}\mathbf{H}(\omega)\mathbf{f} + \mathbf{t}(\omega)^{\dagger}\mathbf{t}(\omega) \end{aligned} \tag{26}$$

where $\mathbf{A}^{\dagger}$ denotes the conjugate transpose of $\mathbf{A}$. The integration of $J(\omega)$ over the whole band $[0, \pi]$ gives the global criterion J:

$$J = \mathbf{f}^{\dagger}\mathbf{\Sigma}\mathbf{f} - \mathbf{f}^{\dagger}\boldsymbol{\alpha} - \boldsymbol{\alpha}^{\dagger}\mathbf{f} + r \tag{27}$$

where:

$$\mathbf{\Sigma} = \int_0^{\pi} \mathbf{H}(\omega)^{\dagger}\mathbf{H}(\omega)\mathrm{d}\omega \tag{28}$$

$$\mathbf{H}(\omega) = \begin{bmatrix} H_1^{(0)}(\mathrm{j}\Omega)\mathbf{e}(\omega) & H_2^{(0)}(\mathrm{j}\Omega)\mathbf{e}(\omega) & \cdots & H_M^{(0)}(\mathrm{j}\Omega)\mathbf{e}(\omega) \\ H_1^{(1)}(\mathrm{j}\Omega)\mathbf{e}(\omega) & H_2^{(1)}(\mathrm{j}\Omega)\mathbf{e}(\omega) & \cdots & H_M^{(1)}(\mathrm{j}\Omega)\mathbf{e}(\omega) \\ \vdots & \vdots & & \vdots \\ H_1^{(M-1)}(\mathrm{j}\Omega)\mathbf{e}(\omega) & H_2^{(M-1)}(\mathrm{j}\Omega)\mathbf{e}(\omega) & \cdots & H_M^{(M-1)}(\mathrm{j}\Omega)\mathbf{e}(\omega) \\ H_1^{(-1)}(\mathrm{j}\Omega)\mathbf{e}(\omega) & H_2^{(-1)}(\mathrm{j}\Omega)\mathbf{e}(\omega) & \cdots & H_M^{(-1)}(\mathrm{j}\Omega)\mathbf{e}(\omega) \\ \vdots & \vdots & & \vdots \\ H_1^{(-(M-1))}(\mathrm{j}\Omega)\mathbf{e}(\omega) & H_2^{(-(M-1))}(\mathrm{j}\Omega)\mathbf{e}(\omega) & \cdots & H_M^{(-(M-1))}(\mathrm{j}\Omega)\mathbf{e}(\omega) \end{bmatrix} \tag{16}$$

$$\boldsymbol{\alpha} = \int_0^{\pi} \mathbf{H}(\omega)^{\dagger}\mathbf{t}(\omega)\mathrm{d}\omega \quad (29)$$

$$r = \int_0^{\pi} \mathbf{t}(\omega)^{\dagger}\mathbf{t}(\omega)\mathrm{d}\omega \quad (30)$$

$\mathbf{\Sigma}$ is a $M \times N$-by-$M \times N$ matrix. $\boldsymbol{\alpha}$ is a $M - by - N$-length column vector and r is a scalar. Moreover, because of the Hermitian characteristic of the matrix $\mathbf{\Sigma}$ and because the digital filter coefficients are real, this leads to:

$$\mathbf{f}^{\dagger}\mathbf{\Sigma}\mathbf{f} = \mathbf{f}^{\mathrm{T}}\mathrm{Re}(\mathbf{\Sigma})\mathbf{f} \quad (31)$$

Also, $\mathbf{f}^{\mathrm{T}}\boldsymbol{\alpha} = \boldsymbol{\alpha}^{\mathrm{T}}\mathbf{f}$, then:

$$J = \mathbf{f}^{\mathrm{T}}\mathrm{Re}(\mathbf{\Sigma})\mathbf{f} - \mathbf{f}^{\mathrm{T}}\boldsymbol{\alpha} - \mathbf{f}^{\mathrm{T}}\boldsymbol{\alpha}^{*} + r \quad (32)$$

The minimum value of this criterion is found by derivating J and by cancelling this function:

$$\frac{\partial J}{\partial \mathbf{f}} = 2\mathrm{Re}(\mathbf{\Sigma})\mathbf{f} - \boldsymbol{\alpha} - \boldsymbol{\alpha}^{*} = 0 \quad (33)$$

The solution can be found by solving the following system:

$$\mathrm{Re}(\mathbf{\Sigma})\mathbf{f} = \mathrm{Re}(\boldsymbol{\alpha}). \quad (34)$$

The solution in a mean square sense is:

$$\mathbf{f} = (\mathrm{Re}(\mathbf{\Sigma})^{\mathrm{T}}\mathrm{Re}(\mathbf{\Sigma}))^{-1}\mathrm{Re}(\mathbf{\Sigma})^{\mathrm{T}}\mathrm{Re}(\boldsymbol{\alpha}) \quad (35)$$

4) Slight oversampling of the input signal: We will show that the performance is better if the input signal is slightly oversampled.

Indeed, assuming that the input signal is band-limited to B, the design of an HFB reconstructing a signal sampled at $2B$ may lead to discontinuities of the ideal synthesis filters frequency responses. With a limited number of coefficients of the synthesis filters, aliasing will be much more important around pulsations $2\pi p/MT$ ($p \in \{-M, ..., M\}$). To decrease aliasing in these areas, we may sample the signal with a slightly higher rate of $2B/\eta$, $0 < \eta < 1$, with η close to 1. Regarding design methods, this is equivalent to assuming that the input signal is limited to the frequency band $[-\eta/T, \eta/T]$. $(1/\eta - 1)$ corresponds to the oversampling ratio.

For a given HFB, oversampling of the input signal improves its performances (see paragraph II-E). But, the performances would be significantly improved if the oversampling is taken into account in the design method. To do that, let's consider the following weighting function.

$$W(\mathrm{j}\Omega) = \begin{cases} 1\,, -\eta\frac{\pi}{T} < \Omega < \eta\frac{\pi}{T} \\ \epsilon\,, \text{otherwise} \end{cases} \quad (36)$$

where $\epsilon \in \mathbb{R}_*^+$, $\epsilon << 1$.

Therefore perfect reconstruction conditions will be:

$$T_p^W(e^{j\omega}) = \begin{cases} ce^{-j\omega\rho}W(\mathrm{j}\Omega)\,, p = 0, \rho \in \mathbb{R}_*^+, c \in \mathbb{R}_* \\ 0 \qquad\qquad\qquad\quad , p \in \mathcal{P} \end{cases} \quad (37)$$

where

$$T_p^W(e^{\mathrm{j}\omega}) = \frac{1}{M}\sum_{m=1}^{M} F_m(e^{\mathrm{j}\omega})H_m\left(\mathrm{j}\Omega - \mathrm{j}\tfrac{2\pi p}{MT}\right)W\left(\mathrm{j}\Omega - \mathrm{j}\tfrac{2\pi p}{MT}\right) \quad (38)$$

with $\omega = \Omega T$.

If (17) and (19) are respectively rewritten as follows:

$$H_m^{(p)}(\mathrm{j}\Omega) = H_m\left(\mathrm{j}\Omega - \mathrm{j}\frac{2\pi p}{MT}\right)W\left(\mathrm{j}\Omega - \mathrm{j}\frac{2\pi p}{MT}\right), \quad (39)$$

$$\mathbf{t}(\omega) = cM\begin{bmatrix} e^{-\mathrm{j}\omega\rho}W(\mathrm{j}\Omega) & 0 & \cdots & 0 \end{bmatrix}^{\mathrm{T}}, \quad (40)$$

(23) or (35) give synthesis filters that take into account the input signal oversampling.

E. Simulation results of HFBs with FIR synthesis filters

Several eight-channel HFBs have been designed from a given analysis filter bank. Considered analysis filter frequency responses are shown in Figure 3. They correspond to the frequency responses of pure resonators whose transfer function is:

$$H_m(s) = \frac{\frac{\Omega_m}{Q_m}s}{s^2 + \frac{\Omega_m}{Q_m}s + \Omega_m^2} \quad (41)$$

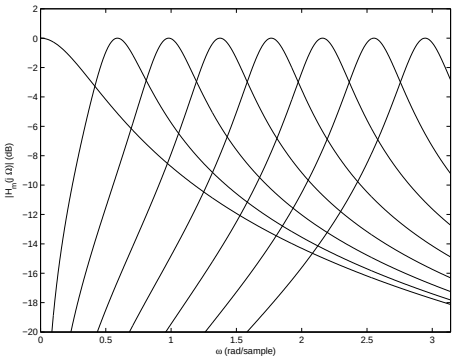

Fig. 3. Analysis filter bank magnitude responses

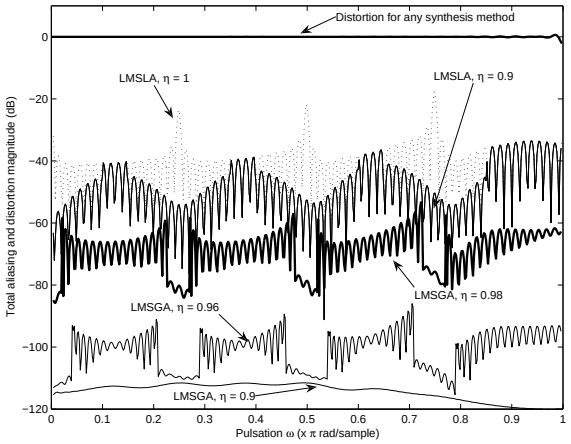

Fig. 4. Total aliasing and distortion magnitudes of HFBs synthesized with the LMSLA and LMSGA methods

where Ω_m is the resonator frequency and Q_m its quality factor. Also, a first order low-pass filter is considered for the lowest frequencies. Its transfer function is:

$$H_1(s) = \frac{\Omega_1}{s + \Omega_1},\ \Omega_1 = \frac{1}{R_1 C_1}, \tag{42}$$

where Ω_1 is the cut-off frequency of the filter. Each synthesis filter has 128 coefficients.

For each synthesis, $K = 512$ pulsation values have been considered for the calculations in $[-\pi, \pi]$ interval. Concerning the LMSGAC method, the integral terms have been calculated by using a rectangular approximation performed on the same points as for the other methods.

Table I gives the main characteristics of all synthesized HFBs. Figure 4 shows the distortion and the total aliasing magnitudes throughout the band for some HFBs. The maximum equivalent resolution expressed in bit may be evaluated by considering the classic 6 dB/bit formula [14]. LMSLA HFB has a mean equivalent resolution of 6 bit only. Moreover total aliasing function peaks are rather high (-17 dB) which degrades the equivalent SFDR (Spurius-Free Dynamic Range) of the HFB A/D converter. If the signal is oversampled by 10%, the equivalent resolution is one bit better and the aliasing peaks are eliminated. With the LMSGAD method and assuming that the signal is slightly oversampled by 2%, the mean equivalent resolution is 11 bit and even 16 bit with an oversampling of 3%. So the LMSGAD method is better than the LMSLA one especially because the input signal oversampling can be taken into account in the LMSGAD method. Compared to LMSGAD, the LMSGAC method gives the same results. However, the LMSGAC method is a little bit more demanding than LMSGAD regarding calculations.

In the next sections, only the LMSGAD method is used.

III. HFB ADAPTATION TO SOFTWARE/COGNITIVE RADIO APPLICATION

In order to give a rough idea of the frequency need, let's imagine a software radio application example that would process GSM, UMTS, WiFi and GPS standards with a single device. To do this, the digitization system should convert the bandwidth [880 MHz, 2.5 GHz]. This means a very wide-band conversion. For cost and energy consumption reasons, it is necessary to minimize the

TABLE I

PERFORMANCES OF LOW-PASS HFBS SYNTHESIZED WITH LEAST MEAN SQUARE METHODS

	LMSLA $\eta = 1$	LMSLA $\eta = 0.9$	LMSGAD $\eta = 1$	LMSGAD $\eta = 0.98$	LMSGAD $\eta = 0.96$	LMSGAD $\eta = 0.9$	LMSGAC $\eta = 1$	LMSGAC $\eta = 0.96$
Mean total aliasing (dB)	-35	-43	-35	-65	-97	-113	-35	-97
Maximum total aliasing (dB)	-17	-33	-17	-53	-86	-111	-17	-86
Mean magnitude distortion (dB)	$-4.8 \cdot 10^{-3}$	$-7.4 \cdot 10^{-4}$	$-7.9 \cdot 10^{-3}$	$8.9 \cdot 10^{-5}$	$3.1 \cdot 10^{-7}$	$4.1 \cdot 10^{-8}$	$-7.9 \cdot 10^{-3}$	$3.1 \cdot 10^{-7}$
Maximum magnitude distortion (dB)	0.63	0.13	0.6	$2.5 \cdot 10^{-2}$	$2.1 \cdot 10^{-4}$	$1.3 \cdot 10^{-5}$	0.6	$2.1 \cdot 10^{-4}$
Mean phase distortion (radian)	$-1.6 \cdot 10^{-3}$	$8.5 \cdot 10^{-5}$	$-1.7 \cdot 10^{-3}$	$1.8 \cdot 10^{-5}$	$2.8 \cdot 10^{-7}$	$4.3 \cdot 10^{-9}$	$-1.7 \cdot 10^{-3}$	$2.8 \cdot 10^{-7}$
Maximum phase distortion (radian)	0.51	$1.7 \cdot 10^{-3}$	0.5	$5.8 \cdot 10^{-3}$	$1.2 \cdot 10^{-4}$	$1.5 \cdot 10^{-6}$	0.5	$1.2 \cdot 10^{-4}$

sampling frequency. To do this, band-pass conversion is one solution.

A. Band-pass HFB

In classical receiver, the A/D conversion is preceded by a downconversion performed by analog mixers. Also, some parallel structures [15] use an analog downconversion. In our work, one of the objectives is to make the analog part as simple as possible, partly by suppressing the downconversion stages. To do that, we chose to make band-pass sampling.

1) Band-pass signal conversion: For a wide-band band-pass signal $x(t)$ bandlimited between $f_{max} - B$ and f_{max}, it is possible to sample at a frequency lower than $2f_{max}$ without aliasing. At the same time, it makes it possible to recover the signal in baseband.

Among the infinite number of terms of (1), we note p_+ the index of the term that corresponds to the signal translated to baseband by the sampling (for positive frequencies). The value of p_+ depends on the input signal band position and on the number of channels M. The Fourier transform of the HFB output is then:

$$Y(e^{\mathrm{j}\omega}) = \frac{1}{T} \sum_{p=p_+-(M-1)}^{p_++(M/2-1)} T_p(e^{\mathrm{j}\omega}) X\left(\mathrm{j}\Omega - \mathrm{j}\frac{2\pi p}{MT}\right) + \sum_{p=-p_+-(M/2-1)}^{-p_++(M-1)} T_p(e^{\mathrm{j}\omega}) X\left(\mathrm{j}\Omega - \mathrm{j}\frac{2\pi p}{MT}\right). \tag{43}$$

Perfect reconstruction conditions become:

$$T_p(e^{\mathrm{j}\omega}) = \begin{cases} ce^{-\mathrm{j}\omega\rho}, p \in \{p_+, -p_+\} \\ 0 \qquad\quad , p \in \mathcal{P}'. \end{cases} \tag{44}$$

$\mathcal{P}' = \{p_+-(M-1), ...p_++(M/2-1)\}\backslash\{p_+\}\bigcup\{-p_+-(M/2-1), ..., -p_++(M-1)\}\backslash\{-p_+\}$.

The minimum sampling rate depends on f_{max} with the relation given in [16]:

$$f_s^{(min)} = \frac{2f_{max}}{n} \tag{45}$$

where n is the floor value of f_{max}/B. This relation is applicable for a single-rate A/D conversion. In the HFB case, on each channel, an overlapping occurs every $2\pi/MT$ (see (1)). So, the minimum sampling frequency is:

$$f_s^{(min)} = \frac{f_{max}M}{n} \tag{46}$$

where n is the floor value of $f_{max}M/(2B)$. Figure 5 shows the minimum sampling frequency for a four-channel HFB A/D converter, an eight-channel HFB A/D converter compared to a single-rate A/D converter. For example, for a set of applications such as GSM, UMTS,

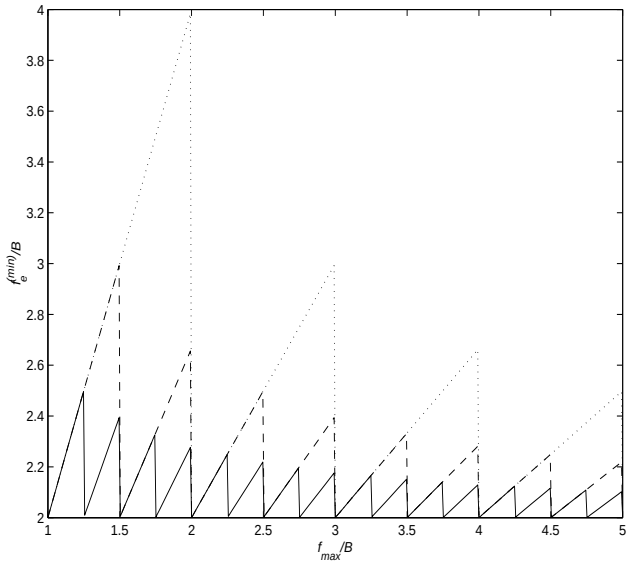

Fig. 5. Minimum sampling frequency for a band-pass signal with four-channel (dashed line) and eight-channel (full line) HFB compared to the Nyquist frequency criterion (dotted line)

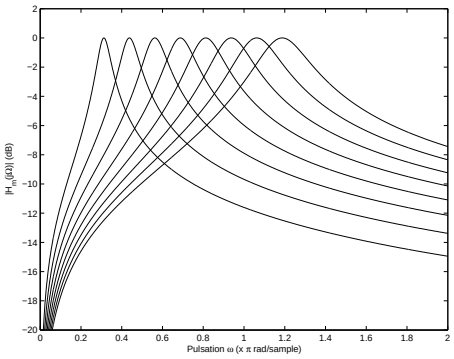

Fig. 6. Analysis filter bank magnitude responses

TABLE II
PERFORMANCES OF A BANDPASS HFB SYNTHESIZED WITH LMSGA ($\eta = 0.97$)

Mean total aliasing (dB)	-68
Maximum total aliasing (dB)	-60
Mean magnitude distortion (dB)	$1.0 \cdot 10^{-4}$
Maximum magnitude distortion (dB)	$2.7 \cdot 10^{-2}$
Mean phase distortion (radian)	$-7.9 \cdot 10^{-6}$
Maximum phase distortion (radian)	$3.4 \cdot 10^{-3}$

GPS and WiFi, corresponding to the band [880 MHz, 2.5 GHz], the Nyquist frequency is 5 GS/s. Considering a four-channel baseband HFB, the output sampling frequency drops to 3.33 GS/s and each A/D converter of each branch would sample at 625 MS/s. With an eight-channel band-pass HFB, the output sampling frequency is 3.33 GS/s too and each A/D converter of each branch can sample at 416 MS/s. Therefore, it relaxes the constraints upon the realization and reduces the power consumption.

The HFB design methods described in Section II-D can easily be adapted for a band-pass sampling as explained in [17].

2) Simulation results of a band-pass HFB: Considering the frequency band [880 MHz, 2.5 GHz], an eight-channel band-pass HFB has been designed. The considered analysis filter frequency responses are shown in Figure 6. They correspond to the frequency responses of pure resonators whose transfer function is given by (41). Quality factors Q_m are identical for all analysis filters and equal to 5. Each synthesis filter has 128 coefficients.

Table II shows detailed performances of an HFB synthesized with the LMSGAD method with an oversampling of 3%. Figure 7 shows the total aliasing and the distortion magnitudes. The total aliasing mean level is equivalent to a resolution of 11 bit.

B. Frequency focusing

Let's suppose that an HFB A/D converter converts a wide band signal at a resolution that could be rather low but sufficient to give a rough idea of the communication channel to be chosen. After the choice of the appropriate communication channel, a higher resolution (together with a narrower bandwidth) might be required. So the software would load a new set of synthesis filter

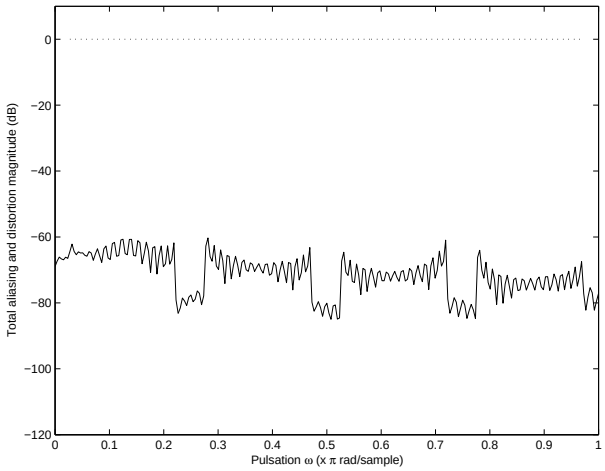

Fig. 7. Band-pass HFB total aliasing (full line) and distortion (dashed line) magnitudes

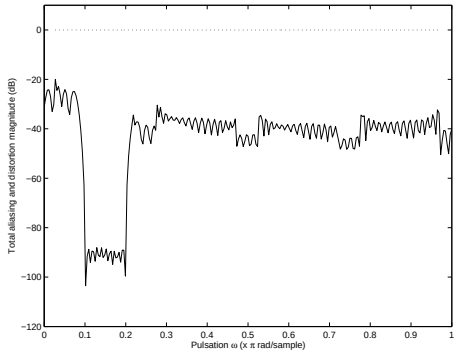

Fig. 8. Band-pass HFB total aliasing (full line) and distortion (dashed line) magnitudes with frequency focusing in $B_f = [0.1/T, 0.2/T]$ band

coefficients to improve the performances in the selected frequency band as illustrated in Figure 1. We present below a method to synthesize synthesis filters adapted to a narrower frequency band [17].

1) Synthesis method: In the following, B_f is the selected frequency band. To synthesize a focused HFB, the main idea is to weight differently the values of the LMSGAD criterion in B_f. This leads to the weighted criterion $\mathbf{\Delta}_{W_f}$.

$$\mathbf{\Delta}_{W_f} = \|\text{diag}(\mathbf{w_f})(\mathbf{H_R f} - \mathbf{t_R})\|^2 \tag{47}$$

where:

$$\mathbf{w_f} = \left[\begin{array}{cccc} \mathbf{w}_d & \mathbf{w}_r & \cdots & \mathbf{w}_r \end{array} \right]^{\mathrm{T}} \tag{48}$$

with:

$$\mathbf{w_d} = \left[\begin{array}{cccc} 1 & 1 & \cdots & 1 \end{array} \right] \tag{49}$$

$$\mathbf{w_r} = \left[\begin{array}{cccc} W_r(\omega_1) & W_r(\omega_2) & \cdots & W_r(\omega_K) \end{array} \right] \tag{50}$$

In (47), $\mathbf{w_d}$ is applied to the distortion term, and $\mathbf{w_r}$ is applied to each aliasing term. $W_r(\omega)$ is a window function that gives weighting to aliasing terms. If this function is equal to 1 where the frequency focusing is desired and a lower value outside that band, it makes it possible to relax constraints in this area and to improve the performances in the selected band. Also, if $W_r(\omega)$ is equal to a value higher than 1 in the selected area, it relaxes constraints upon distortion and therefore, improves aliasing in this area.

2) Simulation results of frequency focusing: The band-pass analysis filter bank in Figure 6 is considered. The previously described synthesis method is used for a frequency focusing on $B_f = [0.1/T, 0.2/T]$. The function $W_r(\omega)$ is equal to 10 in B_f and 0.001 outside. Figure 8 shows the total aliasing and the distortion magnitudes of the resulting HFB. Table III shows that a 48 dB improvement in aliasing characteristics may be achieved within the reduced band B_f (the distortion being almost the same).

Finally, without focusing, the best possible equivalent resolution is 8 bit throughout the B band which may be sufficient for the spectrum sensing mode. With frequency focusing on B_f, the possible resolution becomes 15 bit in B_f which is sufficient for GSM standard.

	in band B_f	out of band
Mean total aliasing (dB)	-90	-34
Maximum total aliasing (dB)	-88	-20
Mean magnitude distortion (dB)	$-3.7 \cdot 10^{-5}$	$2.4 \cdot 10^{-}$
Maximum magnitude distortion (dB)	$1.4 \cdot 10^{-3}$	$1.9 \cdot 10^{-}$
Mean phase distortion (radian)	$-1.0 \cdot 10^{-5}$	$1.7 \cdot 10^{-}$
Maximum phase distortion (radian)	$3.7 \cdot 10^{-4}$	$1.9 \cdot 10^{-}$

TABLE III
HFB PERFORMANCES WITH FREQUENCY FOCUSING IN B_f = $[0.1/T, 0.2/T]$

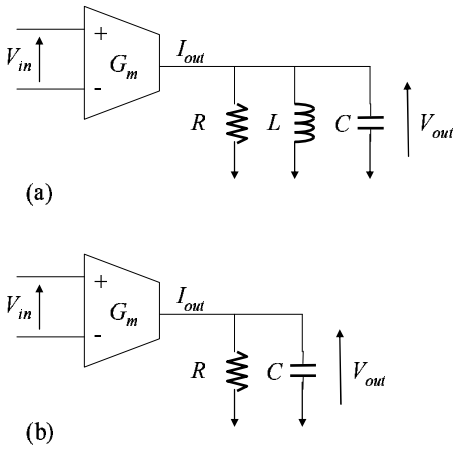

Fig. 9. (a): Resonator filter structure, (b): Low-pass filter structure

C. HFB robustness

The HFB principle is very attractive to enlarge conversion bandwidth. But to become a realistic solution for wide-band applications, HFBs should be robust enough. So, it is necessary to study the HFB sensitivity to imperfections. The first type of imperfections is analog filters errors. Indeed, manufacturing causes errors which make the frequency responses different from the expected ones. The second type of imperfections is caused by the mismatch between A/D converters. This mismatch can be characterized by gain, offset and phase mismatches which are studied in [18], [8] and [19]. The third type of imperfections is digital filtering errors. This consists of errors caused by the quantization of the signal [20] and the quantization of coefficients of the digital filters.

In this work, we study the effect of analog component errors and also the effects of the quantization of digital filter coefficients.

1) Effects of analog components realization errors: This section studies one of the most important drawbacks of implementing A/D converters in HFB structures: the degradation of the HFB performances in the presence of analog components realization errors.

In order to study the influence of realization errors, a realistic example has been chosen. Very simple Gm-LC filters and Gm-C filters (Figure 9) are considered for the band-pass filters and the low-pass filter respectively.

Their transfer functions are similar to those given in (41) and (42). Taking into account realization errors in the previous case, (41) and (42) become:

$$H_m(s) = \frac{\frac{\Omega_m}{Q_m}(1+\Delta_{1m})s}{s^2 + \frac{\Omega_m}{Q_m}(1+\Delta_{1m})s + \Omega_m^2(1+\Delta_{2m})}, \tag{51}$$

$$m \in \{2, ..., M\},$$

$$H_1(s) = \frac{\Omega_1(1+\Delta_{11})}{s + \Omega_1(1+\Delta_{11})}. \tag{52}$$

In (51) and (52) Δ_{1m} and Δ_{11} are the relative errors of the coefficients of the analog filters:

$$\Delta_{1m} = \frac{\varepsilon_{R_m}\varepsilon_{C_m} + \varepsilon_{C_m} + \varepsilon_{R_m}}{1 + \varepsilon_{R_m}\varepsilon_{C_m} + \varepsilon_{C_m} + \varepsilon_{R_m}}, \tag{53}$$

$$\Delta_{2m} = \frac{\varepsilon_{L_m}\varepsilon_{C_m} + \varepsilon_{C_m} + \varepsilon_{L_m}}{1 + \varepsilon_{L_m}\varepsilon_{C_m} + \varepsilon_{C_m} + \varepsilon_{L_m}}, \tag{54}$$

where $m \in \{1, ..., M\}$ and $\varepsilon_{R_m}, \varepsilon_{C_m}$, ε_{L_m} are the relative realization errors of the analog components of the resonators. In order to evaluate the error effects on the distortion and aliasing functions, a Monte Carlo simulation with 1000 trials was performed using (53)

TABLE IV
HFB PERFORMANCES IN THE PRESENCE OF ANALOG REALIZATION ERRORS FOR AN ANALYSIS FILTER BANK USING RESONATORS

Analog errors	Mean aliasing (dB)	Peak aliasing (dB)	Mean distortion (dB)	Peak distortion (dB)
No analog errors	-151	-126	$1.7 \cdot 10^{-9}$	$1.2 \cdot 10^{-6}$
$\varepsilon_{R_m} = 0.01$ $\varepsilon_{L_m} = 0.01$ $\varepsilon_{C_m} = 0.01$	-45	-38	0.0004	0.05

TABLE V
HFB PERFORMANCES IN THE PRESENCE OF ANALOG REALIZATION ERRORS FOR BUTTERWORTH ANALYSIS FILTERS

Analog errors	Mean aliasing (dB)	Peak aliasing (dB)	Mean distortion (dB)	Peak distortion (dB)
No analog errors	-102	-80	$4.6 \cdot 10^{-7}$	$3.3 \cdot 10^{-4}$
$\varepsilon_{R_m} = 0.01$ $\varepsilon_{L_m} = 0.01$ $\varepsilon_{C_m} = 0.01$	-51	-35	0.001	0.07

and (54) to compute analog filter coefficient errors. A four-channel hybrid filter bank was considered with 128-length FIR synthesis filters. Table IV shows the impact of 1% error on passive component values. The aliasing is 106 dB higher than in the case without errors, which is equivalent to a 17 bit resolution loss.

Other filter structures were studied. Higher order Butterworth filters were also considered since they are used as analysis filters in some previous HFB designs [5]. Third order Butterworth filters were taken into account for this study. Again, a Monte Carlo simulation with 1000 trials was performed for a four-channel hybrid filter bank with 128-length FIR synthesis filters. The results are shown in table V. The aliasing is 51 dB higher than in the case without errors, which means a 8 bit resolution loss.

Even with a 1% error on analog components (which is quite optimistic in high frequency technology), the distortion and aliasing functions are degraded so that the equivalent resolution looses at least 8 bit.

2) Effects of digital filter coefficient quantization: In this section, only the errors caused by the quantization of the digital filter coefficients are considered. A fixed arithmetic representation for filter coefficients is supposed to be used and no analog realization errors are taken into account. The error that the quantization of the coefficients produces in the transfer function can be easily evaluated. If the desired transfer function is:

$$F_m(e^{\mathrm{j}\omega}) = \sum_{n=0}^{N-1} f_m(n) e^{-\mathrm{j}\omega n}, \ m \in \{1, 2, ..., M\} \quad (55)$$

then the implemented one is:

$$\widetilde{F}_m(e^{\mathrm{j}\omega}) = \sum_{n=0}^{N-1} \widetilde{f}_m(n) e^{-\mathrm{j}\omega n}. \quad (56)$$

The error introduced by coefficient quantization is:

$$E_m(e^{\mathrm{j}\omega}) = \widetilde{F}_m(e^{\mathrm{j}\omega}) - F_m(e^{\mathrm{j}\omega}) = \sum_{n=0}^{N-1} \epsilon_m(n) e^{-\mathrm{j}n\omega}, \quad (57)$$

where $\epsilon_m(n) = \widetilde{f}_m(n) - f_m(n)$. If a rounding quantization is used, then $\epsilon_m(n) \in \left[-\frac{\Delta}{2}, \frac{\Delta}{2}\right]$, with $\Delta = 2^{-B_q}$ and B_q is the length of the digital word and:

$$\left|E_m(e^{\mathrm{j}\omega})\right| \leq \sum_{n=0}^{N-1} |\epsilon_m(n)| = N\frac{\Delta}{2}. \quad (58)$$

Using (2) and (57), the implemented aliasing and distortion functions are:

$$\widetilde{T}_p(e^{\mathrm{j}\omega}) = T_p(e^{\mathrm{j}\omega}) + \frac{1}{M}\sum_{m=1}^{M} E_m(e^{\mathrm{j}\omega}) H_m\left(\mathrm{j}\Omega - \mathrm{j}\frac{2\pi p}{MT}\right), \tag{59}$$

$$p \in \{-(M-1), ... -1, 0, 1, ..., (M-1)\}.$$

The error appearing in the distortion and aliasing functions can be written as:

$$E_{T_p}(e^{\mathrm{j}\omega}) = \widetilde{T}_p(e^{\mathrm{j}\omega}) - T_p(e^{\mathrm{j}\omega}). \tag{60}$$

Let us assume $|H_m(e^{\mathrm{j}\omega})| \leq 1$ and consider a uniform distribution of the analog filter frequency responses in the working frequency band (e.g. resonators with equally spaced central frequencies). In the passband of each analysis filter, the other filters present important attenuations. Hence:

$$\left|E_{T_p}(e^{\mathrm{j}\omega})\right|_{max} \approx \frac{1}{M}\max_{m,\omega}\left|E_m(e^{\mathrm{j}\omega})\right| = \frac{1}{M} N \frac{\Delta}{2}. \tag{61}$$

(61) is useful after the design phase to decide the necessary number of bit for the FIR coefficient quantization. The error introduced by coefficient quantization (61) must be smaller than the aliasing and distortion errors obtained in the design process.

An eight-channel HFB was considered. Equally spaced, constant band resonators were used as analysis filters. Tests were made for different fixed point formats for coefficient quantization. No deterioration was noticed in the case of the 32-bit fixed point compared to the reference floating point. When 16-bit quantized coefficients are used, (61) results in a predicted error value of -78 dB in the aliasing functions. The same result was obtained in the simulation: the aliasing peak deteriorated from the initial -112 dB to -78 dB due to 16-bit quantization. The simulation results are summarized in Table VI.

Concerning the digital coefficient quantization, it is possible therefore to determine a minimum number of bit in order to limit the aliasing so that the required resolution is obtained. In the given example, if a mean 14-bit resolution is needed, a 16-bit quantization of the digital coefficients is sufficient. Concerning the analog errors, the sensitivity is much more important. A solution could be to measure the analysis filter frequency responses and to calculate the synthesis filters with the LMSGAD method. This could be done by a calibration process or blind estimation. Some results are given in [21], [22] and [23]. [24] proposes an other solution that minimizes reconstruction and realization error energies.

TABLE VI
HFB PERFORMANCES IN THE PRESENCE OF COEFFICIENT QUANTIZATION

	Mean aliasing (dB)	Peak aliasing (dB)	Mean distortion (dB)	Peak distortion (dB)
No quantization	-122	-112	10^{-8}	$1.3 \cdot 10^{-5}$
16 bit fixed point	-88	-78	$1.2 \cdot 10^{-5}$	$6 \cdot 10^{-4}$
32 bit fixed point	-122	-112	10^{-8}	$1.3 \cdot 10^{-5}$

IV. CONCLUSION

In the context of software/cognitive radio applications, HFBs A/D converters are an attractive solution for future A/D conversion systems. First, HFBs make it possible to enlarge the conversion bandwidth. Bandpass HFBs can also be useful to minimize the sampling frequency. This aspect is particularly interesting in the ideal desired scheme of a direct RF conversion. Finally, HFBs offer software controlled versatility. The presented "frequency

focusing" functionality is a way to improve the resolution in a narrower bandwidth by reprogramming the digital part. This is useful if the system needs to perform alternately spectrum sensing and communication.

However, the main drawback of these structures is their sensitivity to the mismatch between the analog and digital parts. The presented HFB design methods optimize the digital filters based on the knowledge of the analog filter frequency responses. This makes it possible to maximally relax constraints on the realization of the analog part. It is clear that an estimation of the analysis filter frequency responses is necessary. A complete study of a calibration method or other solutions such as blind estimation is a topic for further work.

REFERENCES

[1] J. Mitola, "Software radios-survey, critical evaluation and future directions," in *Proceedings of National Telesystems Conference*, May 1992, pp. 13/15–23.

[2] J. Mitola and G. Maguire, "Cognitive Radio: Making Software Radios More Personal," *IEEE Personal Commun. Mag.*, vol. 6, no. 4, pp. 13–18, August 1999.

[3] A. Abidi, "The path to the software-defined radio receiver," *IEEE J. Solid-State Circuits*, vol. 42, no. 5, pp. 954 – 966, May 2007.

[4] S. C. Chan, K. M. Tsui, K. S. Yeung, and T. I. Yuk, "Design and complexity optimization of a new digital if for software radio receivers with prescribed output accuracy," *IEEE Transactions on Circuits and Systems-I: Regular Papers*, vol. 54, no. 2, pp. 351 – 366, February 2007.

[5] S. R. Velazquez, T. Q. Nguyen, and S. R. Broadstone, "Design of hybrid filter banks for analog/digital conversion," *IEEE Transactions on Signal Processing*, vol. 46, no. 4, pp. 956–967, April 1998.

[6] O. Oliaei, "Asymptotically perfect reconstruction in hybrid filter banks," in *Proceedings of IEEE International Conference on Acoustics, Speech, and Signal Processing*, vol. 3, May 1998, pp. 1829 – 1832.

[7] P. Löwenborg, H. Johansson, and L. Wanhammar, "Two-channel digital and hybrid analog/digital multirate filter banks with very low-complexity analysis or synthesis filters," *IEEE Transactions on Circuits and Systems II*, vol. 50, no. 7, pp. 355–367, July 2003.

[8] S. R. Velazquez, "Hybrid filter banks for analog/digital conversion," Ph.D. dissertation, Massachusetts Institute of Technology, June 1997.

[9] S. R. Velazquez, T. Q. Nguyen, S. R. Broadstone, and J. K.Roberge, "A hybrid filter bank approach to analog to digital conversion," in *Proceedings of IEEE International Symposium on Time-Frequency and Time-Scale Analysis*, October 1994, pp. 116–119.

[10] P. Löwenborg, H. Johansson, and L. Wanhammar, "On the frequency response of M-channel mixed analog and digital maximally decimated filter banks," in *Proceedings of European Conference on Circuit Theory and Design*, vol. 1, September 1999, pp. 321–324.

[11] C. Lelandais-Perrault, D. Poulton, and J. Oksman, "Synthesis of hybrid filter banks for A/D conversion with implementation constraints - direct approach," in *Proceedings of IEEE Midwest Symposium on Circuits and Systems*, December 2003.

[12] T. Petrescu, J. Oksman, and P. Duhamel, "Synthesis of hybrid filter banks by global frequency domain least square solving," in *Proceedings of IEEE International Conference on Circuits and Systems*, May 2005.

[13] G. Strang, *Linear algebra and its applications*, 2nd ed. Academic Press, Orlando, 1980.

[14] R. H. Walden, "Analog-to-Digital Converter Survey and Analysis," *IEEE Journal on selected areas in communications*, vol. 17, no. 4, pp. 530–550, April 1999.

[15] S. Mazlouman and S. Mirabbasi, "A frequency-translating hybrid architecture for wide-band analog-to-digital converters," *IEEE Transactions on Circuits and Systems-II: Express Briefs*, vol. 54, no. 7, pp. 576 – 580, July 2007.

[16] R. Vaughan, N. Scott, and D. White, "The theory of bandpass sampling," *IEEE Transactions on Signal Processing*, vol. 39, no. 9, pp. 1973–84, September 1991.

[17] C. Lelandais-Perrault, D. Poulton, and J. Oksman, "Band-pass hybrid filter bank A/D converters with software-controlled bandwidth and resolution," in *Proceedings of IEEE European Conference on Circuit Theory and Design*, vol. I, August 2005, pp. 51–54.

[18] A. Petraglia and S. K. Mitra, "High speed A/D conversion incorporating a QMF bank," *IEEE Transactions on Instrumentation and Measurement*, vol. 41, pp. 427–431, June 1992.

[19] P. Löwenborg, H. Johansson, and L. Wanhammar, "Analysis of gain and timeskew errors in filter bank based A/D converters," in *Proceedings of IEEE Midwest Symposium on Circuits and Systems*, August 2001.

[20] P. Löwenborg and H. Johansson, "Quantization noise in filter bank analog-to-digital converters," in *Proceedings of IEEE Inter-*

national Symposium on Circuits and Systems, vol. 2, May 2001, pp. 601–604.

[21] D. Asemani, J. Oksman, and D. Poulton, "Digital estimation of analog imperfections using blind equalization," in *Proceedings of EUSIPCO*, September 2006.

[22] ——, "Modelling the imperfections of analog circuits using second-order statistics," in *Proceedings of ISCCSP*, March 2006.

[23] D. Asemani, J. Oksman, and P. Duhamel, "Subband architecture for hybrid filter bank a/d converters," *IEEE Journal of Selected Topics in Signal Processing*, vol. 2, no. 2, pp. 191 – 201, April 2008.

[24] M. A. A. Pinheiro, P. B. Batalheiro, A. Petraglia, and M. R. Petraglia, "Improving the near-perfect hybrid filter bank performance in the presence of realization errors," in *Proceedings of IEEE-SP International Conference on Acoustics, Speech, and Signal Processing*, vol. 2, May 2001, pp. 1069–1072.